International Journal of Ecology and Environmental Sciences
www.ecologyjournal.in
Online ISSN: 2664-7133
Received: 27-01-2026, Accepted: 26-02-2026, Published: 13-03-2026
Volume 8, Issue 1, 2026, Page No. 74-86

Groundwater contamination by trace elements and associated health risks in N'Djamena, Chad

Jean-Paul Vicat, Jean-Claude Doumnang Mbaigané, Edith Kadjangaba
Faculty of Exact and Applied Sciences, Laboratory of Geology, University of N'Djamena, Geomorphology, and Remote Sensing, N'Djamena, Chad

Abstract
A large proportion of the population of N'Djamena relies on groundwater from a shallow aquifer that is highly vulnerable to contamination due to inadequate urban sanitation. This study provides the first comprehensive assessment of groundwater quality in the urban area of N'Djamena, based on trace-element concentrations (Li, B, Al, V, Cr, Mn, Co, Ni, Cu, Zn, As, Rb, Sr, Mo, Cd, Ba, Pb, and U), the calculation of pollution indices (Single-Factor Pollution Index, Heavy Metal Contamination Index, Heavy Metal Quality Index, Contamination Index, and Nemerow Pollution Index), and the evaluation of non-carcinogenic and carcinogenic health risks for children and adults through drinking-water ingestion. The results reveal localised contamination, notably by V, Mn, and U, with pollution hotspots mainly associated with the Chari River and the southern section of the Grand Canal. Health risk assessment indicates higher non-carcinogenic risks for children, while carcinogenic risks—primarily driven by arsenic, with minor contributions from nickel—frequently exceed acceptable thresholds, particularly for adults. Although based on groundwater data collected between 2003 and 2005, this study identifies significant patterns of contamination and associated risks, and underscores the need for updated monitoring.

Keywords: Trace elements, urban aquifer, drinking-water, pollution indices, health risk assessment, N'Djamena, Chad

Introduction

N'Djamena, the capital of Chad, is situated in the central part of the Lake Chad Basin, approximately 100 km south of Lake Chad. The geological formations exposed in the region consist entirely of Quaternary deposits (Fig. 1). The population of N'Djamena has increased rapidly, rising from about 560,000 in 2003 to nearly two million in 2026. This rapid demographic growth has led, as observed in many rapidly expanding cities, to a general degradation of environmental conditions. As the national water supply company is unable to meet the growing demand for drinking water, a large proportion of the population relies on groundwater extracted from shallow hand-dug wells tapping the phreatic aquifer.

The groundwater system of N'Djamena consists of a multi-layered aquifer hosted within Quaternary detrital formations composed of alternating clay and sandstone layers overlying a thick Pliocene clay formation (Schneider and Wolff, 1992) [51]. A relatively continuous clay layer of variable thickness (ranging from a few meters to several tens of meters), occurring at depths of around 20 meters, allows the distinction of two main aquifers: an upper aquifer supplying traditional wells and a lower aquifer exploited by boreholes. The lower boundary of the second aquifer is estimated to lie at depths between approximately 60 and 75 m, while a deeper aquifer beneath the Pliocene clay formation remains unexploited. The aquifer exploited is particularly vulnerable due to its limited depth (Moussa *et al*., 2020) [46] and poorly controlled anthropogenic pressures (Kadjangaba, 2007; Bon *et al*., 2021; Idriss Mahamat, 2024) [31, 8, 30]. N'Djamena lacks a centralised sanitation system; wastewater is discharged either into soak pits or directly onto the ground surface and is partly conveyed by the Grand Canal, which runs north to south across the city (Fig. 2), as well as by several smaller channels draining into the Chari River during the rainy season (Doumnang Mbaigané, 2005) [16]. In addition, private latrines are excavated within the urban area down to near the groundwater table (Kadjangaba, 2007) [31], and numerous topographic depressions form semi-permanent ponds that are often filled with urban waste (Doumnang Mbaigané, 2005) [16]. Nitrate contamination has been widely documented in many wells tapping the upper aquifer (Djoret, 2000; Kadjangaba, 2007; Kadjangaba *et al*., 2017, 2018; Deubalbe *et al*., 2021; Edith *et al*., 2022) [15, 31, 32, 33, 13, 18], which are also frequently affected by bacteriological contamination (Tekoum *et al*., 2024) [57]. Results for the deeper aquifer are more variable, with borehole water described either as largely unpolluted (Guideal *et al*., 2010; Kadjangaba *et al*., 2017, 2018) [27, 32, 33] or as locally affected by contamination (Kadjangaba, 2007; Edith *et al*., 2022) [31, 18].

Heavy metal contamination of the N'Djamena aquifer has been investigated only sporadically. A previous study showed that metals mobilised by runoff water leaching contaminated soils tend to accumulate in the unsaturated zone and subsequently migrate towards the groundwater table (Kadjangaba, 2007) [31]. This process highlights the potential for long-term trace element contamination of the aquifer in N'Djamena. The determination of trace elements in groundwater is therefore essential, given their significant impact on drinking-water quality (WHO, 2022) [63]. While some elements, such as manganese, cobalt, copper, zinc, and molybdenum, are essential micronutrients at low concentrations, others as lead, arsenic, and cadmium are toxic even at trace levels and may cause chronic toxicity, carcinogenic effects and neurological disorders following prolonged exposure (WHO, 2022; EPA, 2025) [63, 23]. Accurate quantification of trace elements is thus fundamental for assessing drinking-water safety and associated health risks.

In this context, the present study, based on trace element concentrations in the groundwater of N'Djamena, aims to assess groundwater pollution and potability, and to estimate the non-carcinogenic and carcinogenic health risks associated with groundwater consumption by children and adults.

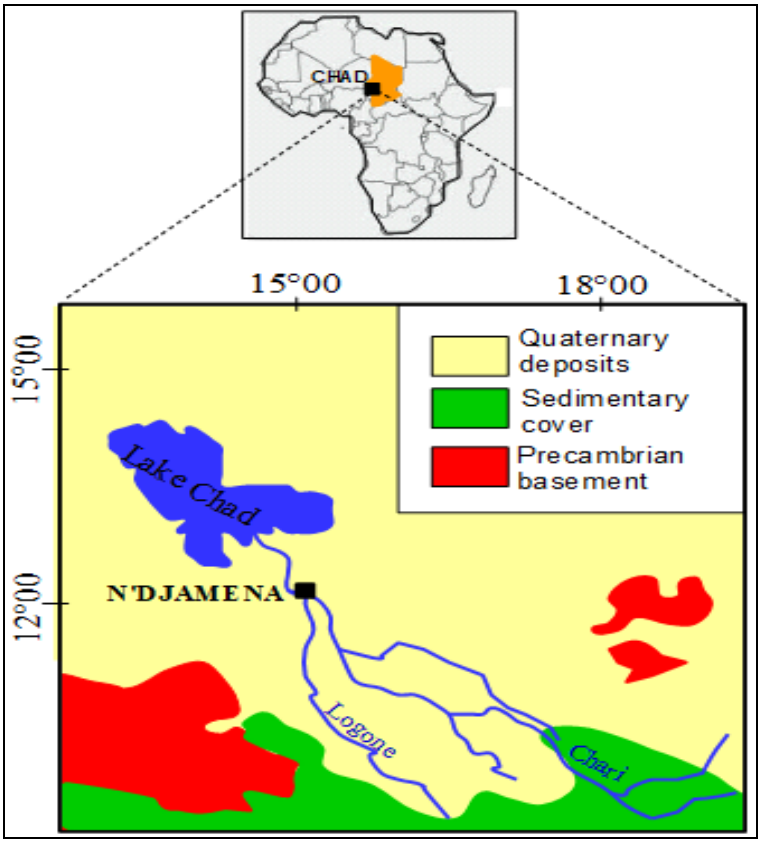

Fig 1: Schematic geological map of the N'Djamena region, after Louis (1970) [38]

Material and Methods

Sampling and analytical methods

Groundwater samples were collected between 2003 and 2005. Twenty-one samples were obtained from wells, two from boreholes, and one from the N'Djamena municipal distribution network (Fig. 2). Samples S–X were collected in 2005, whereas samples 23–52 were collected between 2003 and 2004. Water samples were collected in plastic bottles that had been previously washed, rinsed with distilled water, and finally rinsed with water from the sampling site. Samples were stored in pre-cleaned high-density polyethylene bottles and kept refrigerated until analysis. Trace element analyses—lithium (Li), boron (B), aluminium (Al), vanadium (V), chromium (Cr), manganese (Mn), cobalt (Co), nickel (Ni), copper (Cu), zinc (Zn), arsenic (As), rubidium (Rb), strontium (Sr), molybdenum (Mo), cadmium (Cd), barium (Ba), lead (Pb), and uranium (U)—were performed at the HydroSciences Laboratory in Montpellier (France) using inductively coupled plasma mass spectrometry (ICP-MS) on samples filtered at 0.22 µm. The instrument used was a VG PlasmaQuad PQ2 Turbo+. Analytical accuracy and reproducibility were ensured through calibration with certified reference standards and procedural blanks.

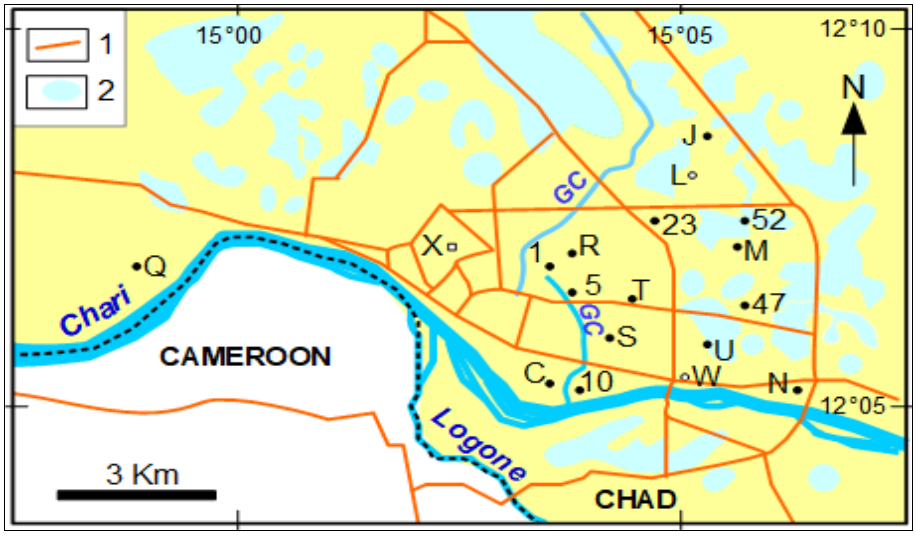

Fig 2: Location of the sampling points in the urban area of N'Djamena. 1: roads and main streets; 2: semi-permanent ponds. Filled circles: wells; open circles: boreholes; open square: tap water. GC: Grand Canal

Statistical analysis of trace elements

Numerous indices have been proposed in the literature to assess water pollution by heavy metals. In this study, the single-factor pollution index was used to compare element concentrations with international drinking-water guideline values. Overall contamination was further assessed using HMCI, HMQI, Cd, and NPI indices. The Heavy Metal Pollution Index (HPI) proposed by Mohan *et al*. (1996) [45] was not calculated because it requires ideal concentrations (Ii) and weighting factors (K), which are inconsistently defined in the literature (Badeenezhad *et al*., 2023; Dey *et al*., 2021; Edet and Offiong, 2002; Kumar and Maurya, 2025) [6, 14, 17, 35]; furthermore, under the commonly adopted simplification (Ii = 0 and K = 1), HPI becomes mathematically equivalent to HMCI. For a comprehensive environmental health risk assessment, we then use both non-carcinogenic and carcinogenic standardized indices.

Single factor pollution index: The Single Factor Pollution Index (Pi) (Dey *et al*., 2021) [14], is equivalent to the Single Pollution Index (Gong *et al*., 2008; Li and Yang, 2008) [26, 36], the Concentration Factor (Cabrera *et al*., 1999) [9], or the Single-Factor Index (Yan *et al*., 2016) [64], which are used to assess soil pollution.

The index is calculated as:

$$Pi = Ci / Si$$

Where Ci is the measured concentration of the element, and Si is its corresponding drinking-water guideline value. A Pi $\leq$ 1 indicates no pollution; 1 < Pi $\leq$ 2 indicates low pollution; 2 < Pi $\leq$ 3 indicates moderate pollution; and Pi > 3 indicates high pollution (Zhaoyong *et al*., 2015; Liu *et al*., 2017; Dey *et al*., 2021) [66, 37, 14]. This approach identifies elements whose elevated concentrations may compromise drinking-water quality. Guideline values are listed in Table 1; when several values were reported in the literature, the most stringent was adopted. The guideline values for B, Li, Al, Cr, Mn, Ni, Cu, Zn, As, Cd, Ba, Pb, and U are from WHO (2022) [63]; V is from OEHHA (2021) [50]; Co from EWG (2023) [24]; Rb from NSF (2018) [48]; Sr from MDH (2019) [42]; and Mo from NHMRC (2011) [47].

Table 1: Guideline values for drinking water (µg L^{-1})

Elements	Li	B	Al	V	Cr	Mn	Co	Ni	Cu	Zn	As	Rb	Sr	Mo	Cd	Ba	Pb	U
Guideline values	10	2400	900	15	50	80	70	70	2000	3000	10	500	3000	50	3	1300	10	30

Heavy metal contamination index.: The heavy metal contamination index (HMCI) was calculated to assess the overall metallic contamination of water. According to Singh *et al*. (2020) [53] and Tiwari *et al*. (2025) [58], HMCI is defined as:

$$= \sum_{i=1}^{n} WcQc / \sum_{i=1}^{n} Wc$$

where Wc=1/Sc and Qc=$\sum_{i=1}^{n} 100 \times Mc/Sc$

Here, Sc represents the WHO maximum permitted concentration for drinking water, and Mc represents the measured concentration. An HMCI value below 100 is generally considered acceptable. For HMCI < 100, water quality is further classified as Low (< 15), Moderate (15–30), or High (> 30) after Singh *et al*. (2020) [53].

Heavy metal quality index: The Heavy Metal Quality Index (HMQI) was used to assess the overall metal contamination of groundwater. The HMQI is calculated according to Zakir *et al*. (2020) [65], Dange *et al*. (2024) [11], and Tiwari *et al*. (2025) [58], by the equation:

$$HMQI = \sum_{i=1}^{n} Mc/Sc$$

Where Mc is the monitored concentration of an element, and Sc is the maximum permissible concentration of the same element. The HMQI is equivalent to the Metal Quality Index (MQI) (Singh *et al*., 2020) [53], the Heavy Metal Evaluation Index (Zakir *et al*., 2020) [65], the Heavy Metal Evaluation Index (Maskooni *et al*., 2020) [41], and the Metal Index (Badeenezhad *et al*., 2023) [6], calculated using the same equation. A value < 1 is considered acceptable for domestic use, whereas a value > 1 indicates unacceptable water quality. Values above 1 are subdivided into low (< 10), medium (10–20), and high (> 20) contamination levels (Maskooni *et al*., 2020) [41].

Contamination Index: The contamination Index (C_d) proposed by Backman *et al*. (1998) [5] assesses overall water contamination based on the concentrations of various heavy metals. The C_d is calculated by the equation:

$$C_d = \sum_{i=1}^{n} CFi \text{ avec } Cfi = \frac{Cai}{Cni} - 1$$

where CF_i represents the contamination factor associated with the i^{th} parameter, Cai is the measured concentration for the i^{th} parameter (µg L^{-1}), and Cni is the maximum allowable concentration for the i^{th} parameter. Elements with concentrations below the upper permissible limit (Cfi < 0) are not taken into account (Backman *et al*., 1998) [5]. To assess the quality of water intended for human consumption, the maximum allowable concentrations are the drinking water guideline values (Table 1). A C_d value of 0 corresponds to unpolluted water, while Cd > 0 corresponds to polluted water, categorized into three grades by Backman *et al*. (1998) [5]: Grade I (low contamination; Cd < 1), Grade II (medium contamination; Cd = 1–3), and Grade III (high contamination; Cd > 3). Because C_d only sums positive contamination factors, it ignores parameters that comply with guideline values. This prevents the dilution effect observed in HMCI and the artificial inflation inherent to unweighted indices such as HMQI. As a result, C_d provides a more realistic appraisal of contamination severity by selectively reflecting only trace elements that exceed drinking-water standards.

Nemerow Pollution Index: The Nemerow Pollution Index (NPI), developed for assessing the overall degree of pollution in soils and sediments (Nemerow, 1991), is also commonly used to evaluate water quality (*Han et al*., 2016; Maskooni *et al*., 2020; Su *et al*., 2022; Chien *et al*., 2024; Meng *et al*., 2024) [29, 41, 54, 10, 43]. The NPI could provide a reasonable interpretation of the heavy metal pollution of the water as a whole. The NPI is calculated by the equation:

$$NPI=[(Pi_{max}^2)/2 + (Pi_{avg}^2)/2]^{1/2}$$

Where max Pi_{max} is the maximum Single Pollution Index among the pollutants, and Pi_{avg} is the mean of Single Pollution Indexes for all the pollutants.

Based on the NPI, water pollution is classified into several levels, with slightly different thresholds depending on the authors. In all cases, an NPI value greater than 1 indicates that the water is polluted, implying that at least one element exceeds its guideline value or that the combined effect of several elements is equivalent to an exceedance. We used the five-level NPI classification proposed by Su *et al.* (2022): Level I (NPI < 0.59; clean, unpolluted), Level II (NPI = 0.59 –0.74; relatively clean), Level III (NPI = 0.74 – 1; good), Level IV (NPI = 1.00 –3.5; polluted), and Level V (NPI ≥ 3.5; heavily polluted).

Like Cd, the NPI provides a more realistic assessment of drinking-water quality than cumulative indices such as HMCI or HMQI, as it integrates both average contamination and the highest individual exceedance. It prevents dilution of a critical contaminant by elements within safe limits and avoids distortion from negligible concentrations, thereby clearly identifying the main drivers of risk.

Non-Carcinogenic and Carcinogenic Risk: The calculation of these indices requires the calculation of the Chronic Daily Intake (CDI). The CDI (mg kg^{-1} day^{-1}), which represents the estimated average daily dose over the relevant exposure period, is calculated using Equation 1:

$$CDI = C \times IR \times EF \times ED / (BW \times AT) \quad (1)$$

where C is the concentration of the contaminant in the water sample, IR is the ingestion rate, ED is the exposure duration, EF is the exposure frequency, AT is the average exposure time, and BW is the body weight. The standard parameter values used to estimate the CDI for children and adults are summarised in Table 2.

The non-carcinogenic risk associated with trace elements in drinking water was assessed using the Hazard Quotient (HQ) approach (EPA, 2011) [21]. For each contaminant, HQ is calculated as*:*

$$HQ = CDI_{NC} / RfD$$

where CDINC is the chronic daily intake for non-carcinogenic effects, and RfD (mg kg^{-1} day^{-1}) is the oral reference dose; the RfD represents the tolerable daily intake of an element that is unlikely to cause adverse health effects over a lifetime. In the case of multiple contaminants, the Hazard Index (HI) represents the combined non-carcinogenic risk resulting from simultaneous exposure to several contaminants and is calculated as the sum of the individual hazard quotients ($HI = \sum HQ_i$). The HI allows assessment of the potential risk associated with the cumulative effects of contaminant mixtures in water, which may be underestimated if only individual HQ values are considered.

Regulatory agencies, including the U.S. EPA and the WHO, generally consider HQ and HI values below 1 to indicate no significant non-carcinogenic risks, whereas values exceeding this threshold suggest the presence of significant concern. The level of risk tends to increase with higher HQ or HI values (Alhagri *et al*., 2024) [3]. More specifically, HI may be classified as negligible (HI < 0.1), low (0.1 ≤ HI < 1), moderate (1 ≤ HI < 4), and high (HI ≥ 4) (Egbueri, 2020; Wator *et al*., 2021) [19, 61]. As hazard quotients are not cumulative over time carcinogenic risk was assessed separately for children and adults. As evidenced by the calculation of AT for CDI_{NC} (Table 2), Equation 1 is equivalent to:

$$CDI_{NC} = C \times IR/BW$$

Using the standard values for IR and BW (Table 2), the CDI_{NC} is always higher for a child than for an adult due to a higher IR/BW ratio for a child compared to an adult. Consequently, children are considered the critical population for non-carcinogenic risk assessment because of their higher exposure dose per unit body weight. Therefore, the absence of significant risk (HQ < 1) for children indicates that non-carcinogenic effects are unlikely to occur in adults under similar exposure conditions.

The carcinogenic risk (CR) was calculated using the following equation:

$$CR = CDI_C \times CSF$$

Where CDI_C is the carcinogenic chronic daily intake calculated using Equation 1 for children and adults according to their respective exposure durations, and CSF (mg kg^{-1} $day^{-1})^{-1}$ is the cancer slope factor. For carcinogenic risk assessment, CDI_C is equivalent to the lifetime average daily dose (LADD), as defined by the EPA (2011) [21]. The averaging time for carcinogenic effects (AT) was set to a lifetime of 70 years (25,550 days) for both children and adults (Table 2).

Table 2: Parameters used for the health risk assessment (after EPA, 2011) [21]

Parameters	Children	Adults	Unit
Ingestion rate (IR)	1	2	L day^{-1}
Exposure duration (ED)	6	30	year
Exposure frequency (EF)	365	365	day $year^{-1}$
Body weight (BW)	15	70	kg
Averaging time for non-carcinogenic risk (AT = ED × EF)	2,190	10,950	day
Averaging time for carcinogenic risk (AT = 70 × EF)	25,550		day

The CR is dimensionless and represents the probability of developing cancer by the age of 70 as a result of exposure to a specific contaminant. For example, a CR of 1.0×10^{-4} indicates an increased lifetime cancer risk of one additional case per 10,000 exposed individuals.

The total cancer risk (TCR) resulting from exposure to multiple carcinogenic trace elements in drinking water is calculated as the sum of the individual CR_i values ($TCR = \sum CR_i$). TCR values within the range of 1×10^{-6} to 1×10^{-4} indicate an acceptable risk level (EPA, 1989; Alhagri *et al*.,

2024) [20, 3]. Values exceeding 1×10^{-4} indicate an unacceptable risk and necessitate the implementation of remedial measures.

In N'Djamena, the standard assumptions for average water consumption (2 L day^{-1} for adults and 1 L day^{-1} for children) may underestimate actual exposure, given the hot semi-arid climate, where mean daily temperatures often exceed 38–40 °C during the dry season. To account for these environmental conditions, the average daily water consumption was estimated at 3 L day^{-1} for adults weighing 70 kg under normal activity levels, and at 1.5 L day^{-1} for a 15 kg child. These estimates are consistent with reported water consumption rates in Nigeria (Kudamnya and Edet, 2024) [34] and Chad (Vicat and Doumnang Mbaigané, 2025) [59].

The RfD and CSF values for the heavy metals are presented in Table 3. The RfDs for Li, B, V, Cr, Mn, Ni, Zn, As, Sr, Mo, Cd, Ba, and U were obtained from the U.S. Environmental Protection Agency's Integrated Risk Information System (IRIS) database (EPA, 2025) [23]. The RfD for Al was taken from ATSDR (2008) [4], and that for Co from Finley *et al*. (2012) [25]. For Cu, we adopted an oral reference dose of 0.04 mg kg^{-1} day^{-1} based on recent evaluative reviews (Taylor *et al*., 2023) [56], noting that the U.S. EPA's Integrated Risk Information System (IRIS) database does not currently list an official RfD for copper. As no RfD for Pb is available in the IRIS database, a value of 0.0015 mg·kg^{-1}·day^{-1} was adopted, in agreement with recent studies (Bhushan *et al*., 2025; Shakoor *et al*., 2025) [7, 52]. This value is more representative of current risk assessment practices than older estimates such as 0.014 mg kg^{-1} day^{-1} (Wator *et al*., 2021) [61], 0.0035 mg kg^{-1} day^{-1} (Dashtizadeh *et al*., 2019) [12], or the very conservative value of 0.00036 mg kg^{-1} day^{-1} (Alhagri *et al*., 2024) [3]. No RfD for Rb is available in the IRIS database; therefore, we adopted the RfD value of 0.02 mg kg^{-1} day^{-1} reported in the Provisional Peer-Reviewed Toxicity Values database (EPA, 2016) [22].

Table 3: RfD (mg kg^{-1} day^{-1}) and CSF (mg kg^{-1} $day^{-1})^{-1}$) for the analysed elements. NA: not available

Element	RfD	CSF
Li	0.002	*NA*
B	0.2	*NA*
Al	1	*NA*
V	0.009	*NA*
Cr	0.0009	0.27
Mn	0.14	*NA*
Co	0.03	*NA*
Ni	0.02	1.7
Cu	0.04	*NA*
Zn	0.3	*NA*
As	0.00006	32
Rb	0.02	*NA*
Sr	0.6	*NA*
Mo	0.005	*NA*
Cd	0.0005	6.3
Ba	0.2	*NA*
Pb	0.0015	0.0085
U	0.003	*NA*

The CSFs for Cr and As were obtained from the IRIS database (EPA, 2025) [23]. For inorganic arsenic, the most recent oral CSF, 32 (mg kg^{-1} $day^{-1})^{-1}$, was used (EPA, 2025) [23]. This value, derived from a Bayesian meta-analysis of epidemiological studies on bladder and lung cancers, is substantially higher than the previously used value of 1.5 (mg kg^{-1} $day^{-1})^{-1}$. The use of this updated CSF, as applied in recent studies (Luo *et al*., 2026) [39], reflects the current scientific consensus and may result in higher estimated cancer risks compared with earlier assessments. As no CSF for Ni is available from the EPA, we adopted the more protective value of 1.7 (mg kg^{-1} $day^{-1})^{-1}$ reported by Akintola *et al*. (2025) [2], compared with 0.84 (mg kg^{-1} $day^{-1})^{-1}$ reported by Alhagri *et al*. (2024) [3]. For Cd, the CSF reported in the literature varies widely (Miletic *et al*., 2023) [44] due to the absence of an official CSF from regulatory agencies. In this study, we adopted a conservative approach by using the higher value of 6.3 (mg kg^{-1} $day^{-1})^{-1}$ (Alhagri *et al*., 2024) [3] to avoid underestimating potential health risks. For Pb, we used a CSF value of 0.0085 (mg kg^{-1} $day^{-1})^{-1}$ from OEHHA (2009) [49], which has been commonly applied in recent studies (Alhagri *et al*., 2024; Gwira *et al*., 2024; Stephen *et al*., 2024) [3, 28, 54].

Regarding As, the RfD and CSF established by the U.S. EPA are defined for inorganic arsenic. Because ICP-MS analyses measure total dissolved arsenic, the concentration must be adjusted to reflect the predominance of inorganic species in natural waters (≈ 90%) (WHO, 2001; Mandal and Suzuki, 2002) [62, 40].

Results and discussion

Trace element concentrations are presented in Table 4. Samples S–X correspond to new data, whereas samples 23–52 were taken from Kadjangaba (2007) [31]; for all samples, pollution indices and risk assessments were calculated for the first time in this study.

Table 4: Groundwater trace element concentrations (μg L^{-1})

Sample	S	J	C	N	T	M	R	Q	W	L	U	X
Date	2004-04	2004-04	2004-04	2004-04	2004-04	2004-04	2004-04	2004-04	2004-04	2004-04	2004-04	2004-04
Li	0.266	0.77	0.28	0.50	0.37	0.87	1.03	0.24	0.23	0.96	2.73	0.97
B	4.49	11.41	7.19	4.14	6.93	9.05	7.69	4.04	4.26	8.86	5.54	7.48
Al	18.83	19.95	29.94	4.20	10.48	18.03	5.22	2.03	1.57	0.73	7.10	7.47
V	19.07	0.69	0.25	0.10	13.12	2.01	0.38	1.63	0.34	1.30	0.37	4.67
Cr	0.85	1.00	0.75	0.77	0.80	0.58	0.96	0.69	0.44	0.66	0.98	0.83
Mn	73.47	108.93	251.84	54.85	26.39	74.80	118.55	69.41	195.74	39.05	43.95	52.33
Co	0.20	0.47	0.85	0.78	0.35	0.78	0.73	0.80	0.58	0.52	0.65	0.07
Ni	1.42	1.06	1.60	0.45	0.93	1.88	1.18	0.73	0.65	0.85	2.61	0.66
Cu	0.99	0.93	1.79	0.79	1.21	1.17	0.96	1.07	0.81	1.35	1.67	3.87
Zn	17.49	15.50	17.10	7.18	87.70	50.74	20.03	11.03	667.76	16.06	28.64	592.77
As	1.70	0.06	1.69	0.69	0.87	0.05	0.71	1.88	2.85	0.24	0.15	1.23
Rb	2.47	3.82	4.13	5.20	3.49	6.46	5.73	1.52	2.08	4.23	15.32	4.60
Sr	230.50	358.28	119.98	126.28	314.08	89.86	293.74	202.92	152.65	113.07	219.58	251.80
Mo	0.29	0.14	0.41	0.34	1.25	0.41	0.64	0.20	0.25	0.21	0.94	0.73
Cd	0.11	0.08	0.22	0.66	0.28	0.07	0.41	0.07	0.21	0.04	0.32	0.04
Ba	213.44	343.82	100.53	216.14	242.64	190.49	482.56	371.32	97.40	233.26	359.88	185.83
Pb	0.12	0.19	0.35	0.08	0.18	0.15	0.14	0.12	0.29	0.12	0.16	2.19
U	0.92	2.47	0.06	0.15	1.00	0.07	0.95	1.06	0.02	0.06	0.24	0.30

Table 1, continued

Sample	23	23a	1	1a	1b	5	5a	5b	47	47 a	52	10
Date	2004-01	2003-11	2003-01	2003-11	2004-01	2003-03	2003-11	2004-01	2003-11	2004-01	2003-11	2003-03
Li	0.754	0.748	0.792	0.929	0.501	1.876	2.081	2.148	0.549	0.583	1.36	1.845
B	15.267	14.289	8.938	8.945	69.953	6.673	8.973	9.433	8.357	9.785	17.784	4.894
Al	16.759	10.625	8.062	6.35	480.61	10.117	7.418	5.301	6.783	7.764	9.944	24.884
V	1.975	2.185		0.564	2.375		5.133	4.067	1.417	1.573	5.972	
Cr	0.885	0.832	0.708	0.831	1.703	0.096	2.716	3.249	1.166	1.193	1.233	0.438
Mn	50.352	77.491	247.84	94.768	57.774	178.61	227.61	161.93	187.2	222.34	27.053	593.55
Co	0.207	0.254	1.041	0.613	1.023	0.355	0.192	0.179	0.855	1.378	0.246	3.648
Ni	5.637	1.319	2.247	1.612	5.862	1.666	1.873	1.647	12.821	24.48	1.574	1.918
Cu	1.222	0.882	2.178	1.151	5.798	3.061	1.634	1.409	1.193	1.595	1.161	1.641
Zn	13.253	8.34	10.87	14.179	1335.1	7.848	111.44	18.834	28.015	38.737	19.599	8.712
As	0.156	0.2	1.081	0.446	1.19	1.645	1.062	0.756	0.159	0.195	0.194	1.57
Rb	3.58	3.943	6.399	5.823	2.326	2.463	3.172	3.759	11.588	12.021	5.034	2.029
Sr	294.43	338.72	341.53	299.69	252.05	658.12	552.64	590.6	436.47	615.25	224.21	128.36
Mo	0.286	0.269	0.661	0.541	0.387	1.092	1.087	0.987	1.64	1.724	0.218	0.365
Cd												
Ba	262.07	313.36	565.79	470.99	164.68	942.77	999.57	1134.7	181.85	182.69	153.03	195.4
Pb	0.193	0.106	0.245	0.123	2.559	0.567	0.148	0.154	0.127	0.174	0.119	0.273
U	2.183	2.842	1.212	1.161	0.484	6.487	9.074	11.068	51.885	56.118	0.227	0.263

Single factor pollution index: Table 5 summarises the results of the calculation of the single factor pollution index (Pi), indicating for each sample the number of Pi values in each pollution class and the corresponding contaminant elements. Occasionally, positive Pi values highlight contamination by V, Mn, and U. V contamination is low ($1 < Pi \leq 2$) and affects only well S (Fig. 3). Mn contamination is low in wells J, R, and 1a, moderate ($2 < Pi \leq 3$) in borehole W and wells 5 and 47, and high ($Pi > 3$) in wells C, 1, and 10. For wells 23, 5, and 47, which were sampled several times, Pi values greater than 1 attributed to Mn and U remain similar from one year to another, whereas in well 1, Mn concentrations decrease markedly over time (from $Pi > 3$ in January 2003 to $Pi \leq 1$ in January 2004; Table 4). This marked temporal decrease in Mn concentration, unlike that observed in neighbouring wells, probably reflects site-specific processes, such as progressive oxidation of Mn^{2+} induced by local variations in redox potential and/or well-related factors such as increased pumping frequency or disturbance of sediments within the well, rather than a regional change in groundwater quality.

As evidenced by Table 5, contamination is mainly driven by Mn. The Mn contamination is attributed to the accumulation of domestic waste in the urban area, particularly in ponds and in the Grand Canal. Such waste includes large quantities of discarded batteries, which contribute to elevated Mn concentrations in soils (463–835 ppm; Kadjangaba, 2007 [31]) with leachates subsequently migrating into the groundwater system. Given the geological context, the isolated enrichments of V in well S and U in well 47 may

indicate localised anthropogenic contamination rather than a regional geogenic source. Vanadium enrichment could be linked to urban waste and fuel-related pollution, whereas uranium enrichment may be associated with urban waste and the use of phosphate fertilisers.

Table 5: Single factor pollution index (Pi). The number of Pi values per pollution class is indicated for each sample, followed by the symbol of the element responsible for the contamination in parentheses

Samples	Pi ≤1	1< Pi ≤2	2 < Pi ≤ 3	Pi >3	Pi values
S	17	1 (V)	0	0	1.3
J	17	1 (Mn)	0	0	1.4
C	17	0	0	1 (Mn)	3.1
N	18	0	0	0	<1
T	18	0	0	0	
M	18	0	0	0	
R	17	1 (Mn)	0	0	1.5
Q	18	0	0	0	
W	17	0	1 (Mn)	0	2.4
L	18	0	0	0	
U	18	0	0	0	
X	18	0	0	0	
23	18	0	0	0	
23a	18	0	0	0	
1	17	0	0	1 (Mn)	3.1
1a	17	1 (Mn)	0	0	1.2
1b	18	0	0	0	
5	17		1 (Mn)	0	2.2
5a	17		1 (Mn)	0	2.9
5b	17		1 (Mn)	0	2.0
47	16	1 (U)	1 (Mn)	0	1.7 (U) 2.3 (Mn)
47a	16	1 (U)	1 (Mn)	0	1.9 (U) 2.8 (Mn)
52	18	0	0	0	
10	17	0	0	1 (Mn)	7.4

The values of the Heavy Metal Contamination Index (HMCI), Heavy Metal Quality Index (HMQI), Contamination Index (C_d), and Nemerow Pollution Index (NPI) are presented in Table 6.

Table 6: HMCI, HMQI, C_d, and NPI values. For wells sampled multiple times, the mean value was used.

Samples	HMCI	HMQI	Cd	NPI
S	16.01	2.79	0.27	0.91
J	5.19	2.09	0.36	0.97
C	10.84	3.70	2.15	2.23
N	11.71	1.31	0.00	0.49
T	13.40	1.87	0.00	0.62
M	4.90	1.49	0.00	0.66
R	10.67	2.42	0.48	1.05
Q	6.19	1.66	0.00	0.62
W	10.96	3.26	1.45	1.73
L	3.69	0.99	0.00	0.35
U	9.36	1.48	0.00	0.39
X	9.56	1.92	0.00	0.47
23	4.18	1.56	0.00	0.57
1	6.65	2.88	0.76	1.19
5	11.00	4.33	1.37	1.68
47	13.78	5.25	2.36	1.82
52	5.96	1.19	0.00	0.29
10	16.04	8.12	6.42	5.26

Heavy metal contamination index: Most wells exhibit low HMCI (HMCI < 15), while two wells (S, 10) show moderate contamination (15 ≤ HMCI ≤ 30) (Table 6). These values are far below the commonly adopted quality threshold (HMCI = 100) and therefore suggest good water quality. However, this assessment contrasts with the pollution index (Pi), which in certain cases classifies the water as unsuitable for human consumption. This discrepancy arises from the HMCI calculation method. The HMCI is a weighted average ($\sum WcQc / \sum Wc$) in which elements present at safe levels ($Mc \ll Sc$) contribute very small WcQc values. The cumulative weight of numerous such elements analysed (Li, B, Al, Cr, Co, Ni, C, Zn, As, Rb, Mo, Cd, Ba) substantially reduces the influence of trace elements such as V, Mn, Sr, and U that sometimes exceed drinking-water guideline values.

Contamination Index: Several water samples (N, T, M, Q, L, U, X, 23, 52) show Cd = 0 (Table 6), indicating that none of the analysed trace elements exceed their permissible limits. The remaining samples exhibit variable C_d values, ranging between 0 and 1 (samples S, J, R, 1), between 1 and 3 (samples C, W, 5, 47), and > 3 (sample 10), corresponding to low, moderate, and high contamination levels, respectively, according to Backman *et al*. (1998) [5].

Nemerow Pollution Index: The NPI values (Table 6) show that several samples (N, L, U, X, 23, 52) fall into Class I (unpolluted), whereas others correspond to relatively clean waters (Class II: T, M, Q) or good-quality waters (Class III: S, J). In contrast, samples C, R, W, 1, 5, and 47 fall into Class IV (polluted), and sample 10 into Class V (heavily polluted), according to Su *et al*. (2022) [55].

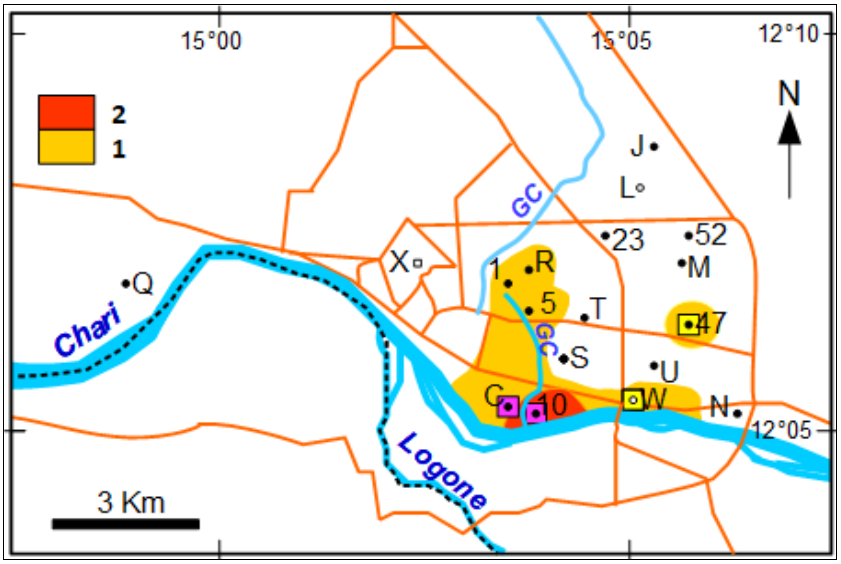

Fig 3: Spatial distribution of polluted zones. Yellow and magenta squares indicate moderate and high pollution levels, respectively, based on Pi values. (1) C_d classified as Grade II and NPI as Level IV; (2) C_d classified as Grade III and NPI as Level V

The spatial distribution of moderate ($2 < Pi \leq 3$) to high ($Pi > 3$) Pi values, together with C_d (Grades II–III; medium and high contamination) and NPI values (Levels IV and V; polluted and heavely polluted) (Fig. 3), clearly delineates the two most contaminated zones. One coincides with the southern part of the Grand Canal and extends upstream along the Chari River, while the other, more limited, is located around well 47. These zones correspond to areas where soils are heavily contaminated by trace metals—particularly the ponds surrounding well 47, those near well W, and the southern part of the Grand Canal (Kadjangaba, 2007) [31]—as well as to an intensive market gardening area along the Chari River. Metal-enriched leachates generated in these contaminated soils may therefore infiltrate and migrate towards the shallow aquifer, contributing to the observed groundwater contamination.

Table 7: HQ and HI assessment results for children and adults. Minimum (MIN), mean, and maximum (MAX) HQ values are reported. *n* represents the number of analyses for which the risk is non-negligible (HQ > 0.1). For wells sampled multiple times, the average HI value was used

	Children HQ				Adults HQ					HI	
	MIN	**MEAN**	**MAX**	***n***	**MIN**	**VM**	**MAX**	***n***	**Samples**	**Children**	**Adults**
Li	0.012	0.049	0.137	3	0.005	0.021	0.059	0	S	3.15	1.35
B	0.000	0.000	0.002	0	0.000	0.000	0.001	0	J	0.68	0.29
Al	0.000	0.003	0.048	0	0.000	0.001	0.021	0	C	2.99	1.28
V	0.001	0.037	0.212	2	0.000	0.016	0.091	0	N	1.47	0.63
Cr	0.011	0.113	0.361	9	0.005	0.048	0.155	2	T	1.91	0.82
Mn	0.019	0.096	0.424	9	0.008	0.041	0.182	1	M	0.44	0.19
Co	0.000	0.002	0.012	0	0.000	0.001	0.005	0	R	1.76	0.75
Ni	0.002	0.016	0.122	1	0.001	0.007	0.052	0	Q	3.27	1.40
Cu	0.002	0.004	0.014	0	0.001	0.001	0.004	0	W	4.84	2.08
Zn	0.002	0.044	0.445	3	0.001	0.019	0.191	1	L	0.69	0.30
As	0.081	1.297	4.268	22	0.035	0.556	1.829	21	X	2.60	1.11
Rb	0.008	0.025	0.077	0	0.003	0.011	0.033	0	U	0.85	0.36
Sr	0.015	0.050	0.110	2	0.006	0.021	0.047	0	23	0.79	0.34
Mo	0.003	0.013	0.034	0	0.001	0.005	0.015	0	1	2.17	0.93
Cd	0.007	0.042	0.132	1	0.003	0.018	0.057	0	5	3.21	1.37
Ba	0.049	0.179	0.567	15	0.021	0.077	0.243	6	47	2.72	1.17
Pb	0.005	0.025	0.171	2	0.002	0.011	0.073	0	52	0.73	0.31
U	0.001	0.209	1.871	5	0.000	0.089	0.802	4	10	3.11	1.33

Non-carcinogenic Risk: Table 7 presents the Hazard Quotient (HQ) and Hazard Index (HI) values for children and adults through drinking-water ingestion. According to the HQ values, As is the main contributor to non-carcinogenic risk in the analysed water samples. This dominance reflects the updated RfD for As reported in the IRIS database (6×10^{-5} mg kg^{-1} day^{-1}), which incorporates recent epidemiological evidence of cardiovascular and metabolic effects (EPA, 2025) [23]. This value is considerably more conservative than the value commonly used in previous groundwater risk assessment studies (3×10^{-4} mg kg^{-1} day^{-1}). Consequently, although arsenic concentrations are well below the drinking-water guideline value (10 µg L^{-1}), As dominates the non-carcinogenic risk due to its very low RfD.

The HI values range from 0.44 to 4.84 for children and from 0.19 to 2.08 for adults; No sample presents a negligible risk. For children, six samples (J, M, L, U, 23, 52) present a low risk ($0.1 \leq HI < 1$), whereas the remaining samples exceed the acceptable threshold (HI = 1), including eleven samples (S, C, N, T, R, Q, X, 1, 5, 47, 10) with moderate risk ($1 \leq HI < 4$) and one sample (W) with high risk ($HI \geq 4$). The spatial distribution of HI values for children (Fig. 4) shows that the area along the Chari River and the Grand Canal presents a moderate risk, with a high-risk hotspot at borehole W. In contrast, wells J, 23, 52, and M, together with borehole L, located in the north-eastern part of the urban area, show a low risk.

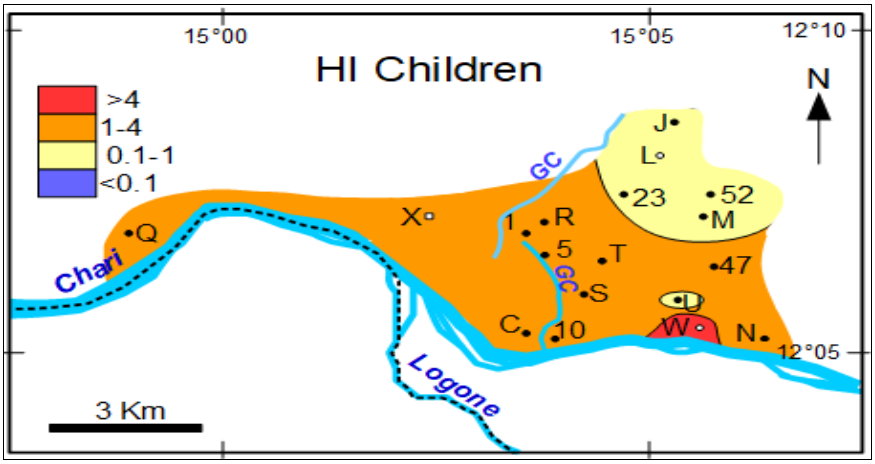

Fig 4: Spatial distribution of HI values for children. Non-carcinogenic risk classification: negligible (HI < 0.1), low ($0.1 \leq HI < 1$), moderate ($1 \leq HI < 4$), and high ($HI \geq 4$)

For adults, ten samples (J, N, T, M, R, L, U, 23, 1, 52) indicate low risk ($0.1 \leq HI < 1$) and eight (S, C, Q, W, X, 5, 47, 10) moderate risk ($1 \leq HI < 4$). The spatial distribution of HI values for adults (Fig. 5) highlights a moderate-risk zone along the Chari River bank, including the southern part of the Grand Canal and the area near well 47. Compared with the distribution observed for children, the low-risk zone is much more extensive towards the west and south, where it reaches the Chari River upstream of borehole W.

As expected, the higher HI and HQ values observed in children compared with adults indicate greater susceptibility to non-carcinogenic risks from trace elements, due to their higher intake per unit body weight.

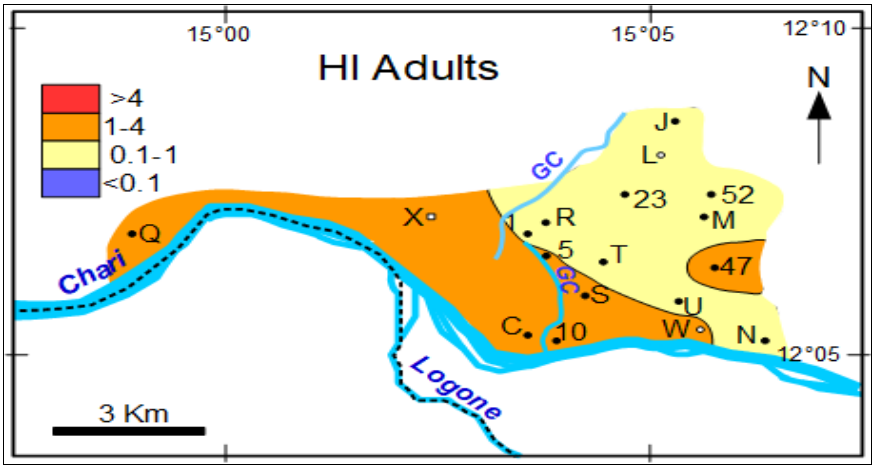

Fig 5: Spatial distribution of HI values for adults. Same legend as Fig. 4

Carcinogenic Risk: Table 8 presents the CR values for children and adults through drinking-water ingestion. All analysed samples exhibit negligible ($CR \leq 1 \times 10^{-6}$) or acceptable ($1 \times 10^{-6} < CR \leq 1 \times 10^{-4}$) risk levels for Cr, Cd, and Pb. For children, two samples show unacceptable risk levels for Ni and fifteen samples for As. For adults, four samples show unacceptable risk levels for Ni and eighteen samples for As. Consistent with these results, As is the main contributor to lifetime cancer risk despite concentrations below the drinking-water guideline value, due to its revised high CSF ($(32 \text{ (mg kg}^{-1} \text{ day}^{-1})^{-1}$).

Table 8: CR assessment results for children and adults. Minimum (MIN), mean, and maximum (MAX) HQ values are reported. *n* represents the number of analyses for which the risk is unacceptable (CR > 1 × 10

	Children CR				Adults CR			
	MIN	MEAN	MAX	*N*	MIN	MEAN	MAX	*n*
Cr	4.1E-07	4.3E-06	1.4E-05	0	8.8E-07	9.2E-06	3.0E-05	0
Ni	6.6E-06	4.7E-05	3.6E-04	2	1.4E-05	1.0E-04	7.6E-04	4
As	1.3E-05	2.1E-04	7.0E-04	15	3.2E-05	5.1E-04	1.7E-03	18
Cd	1.9E-06	1.1E-05	3.5E-05	0	4.3E-06	2.3E-05	7.4E-05	0
Pb	5.8E-09	2.7E-08	1.9E-07	0	1.2E-08	5.8E-08	4.0E-07	0

Table 9: TCR assessment results for children and adults through drinking-water ingestion. For wells sampled multiple times, the average TCR value was used.

Sample	Children TCR	Adults TCR
S	4.50E-04	1.06E-03
J	3.74E-05	8.33E-05
C	4.55E-04	1.07E-03
N	2.15E-04	5.01E-04
T	2.46E-04	5.78E-04
M	4.68E-05	1.03E-04
R	2.18E-04	5.09E-04
Q	4.81E-04	1.14E-03
W	7.25E-04	1.72E-03
L	7.62E-05	1.77E-04
X	9.50E-05	7.53E-04
U	3.19E-04	2.12E-04
23	9.83E-05	2.21E-04
1	2.75E-04	6.44E-04
5	3.19E-04	7.51E-04
47	3.21E-04	6.97E-04
52	7.61E-05	1.75E-04
10	4.17E-04	9.87E-04

Table 9 presents theTCR values for children and adults through drinking-water ingestion. TCR values for children range from 3.74×10^{-5} to 7.25×10^{-4}, and for adults from 8.33×10^{-5} to 1.72×10^{-3}. For children, water from wells J, M, 23, 52, borehole L, and tap water X shows an acceptable risk ($1 \times 10^{-6} < TCR < 1 \times 10^{-4}$). The remaining wells present an unacceptable risk ($1 \times 10^{-4} < TCR < 5 \times 10^{-4}$). Borehole W presents the highest risk ($TCR = 7.25 \times 10^{-4}$). The spatial distribution of TCR values for children (Fig. 6) indicates that acceptable risk is confined to the north-eastern part of the city; the municipal tap water sample (X) also presents an acceptable risk. The rest of the urban area shows an unacceptable risk, particularly along the banks of the Chari River near borehole W.

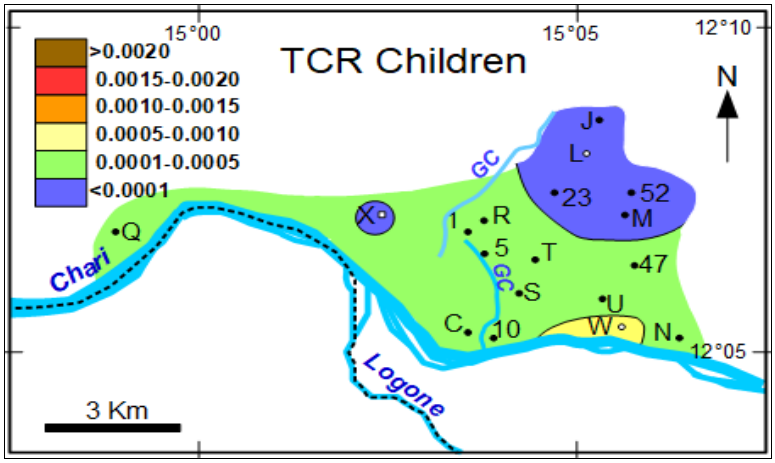

Fig 6: Spatial distribution map of TCR values for children in the study area

For adults, only well J presents an acceptable risk, while the other wells, borehole L, and tap water X show an unacceptable risk. Wells M, U, 23, 52, and borehole L have TCR values between 1×10^{-4} and 5×10^{-4}. TCR values for wells N, T, R, 1, 5, 47, and 10, as well as tap water X, are higher ($5 \times 10^{-4} < TCR < 1 \times 10^{-3}$). Wells S, C, and Q show higher TCR values ($1 \times 10^{-3} < TCR < 1.5 \times 10^{-3}$), and borehole W presents the highest risk ($TCR = 1.72 \times 10^{-3}$). For adults, except the far north-east, the entire urban area exhibits an unacceptable risk, increasing towards the south-

west (Fig. 7). Three high-risk zones are located along the Chari River: downstream near well Q, in the central area near southern part of the Grand Canal, and upstream near borehole W.

The higher CR and TCR values observed in adults compared with children reflect the longer exposure duration considered in the risk assessment.

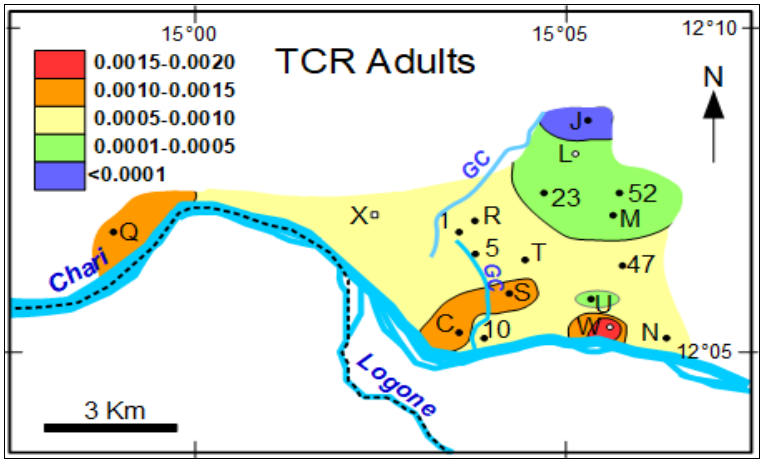

Fig 7: Spatial distribution map of TCR values for adults in the study area

For the risk assessment, an alternative scenario incorporating the lower Cd CSF reported in the literature (0.38 (mg·kg^{-1}·day^{-1})$^{-1}$; Abdelhalim *et al*., 2022; Stephen *et al*., 2024) [1, 54] does not modify the results, as the estimated risk is primarily driven by As owing to its high CSF. A second alternative scenario was tested using an upper-bound assumption in which the inorganic arsenic fraction was uniformly set at 70% for all samples. This assumption accounts for the potential influence of urban effluents and latrine leachates infiltrating the shallow aquifer of N'Djamena (Djoret, 2000; Kadjangaba, 2007) [15, 31], which may enhance microbial methylation processes and increase the proportion of organic As (Wang, 2022) [60]. This scenario yields slightly lower index values but does not materially affect the overall interpretation.

Conclusion

Most trace-element concentrations comply with drinking-water guideline values; however, locally elevated levels of Mn, V, and U contribute to pollution indices indicating groundwater degradation. Health risk assessment reveals significant non-carcinogenic risks for children and carcinogenic risks frequently exceeding acceptable thresholds for both children and adults, particularly due to As.

This study provides the first comprehensive assessment of trace-element contamination and related health risks in the shallow groundwater of N'Djamena. Although based on samples collected between 2003 and 2005, it establishes a valuable baseline prior to the city's rapid expansion over the last two decades and can serve as a reference for evaluating subsequent changes in groundwater quality. Indeed, a large proportion of the population still relies on shallow wells and private boreholes, particularly in peri-urban areas not connected to the municipal supply network. Moreover, inadequate sanitation and uneven waste collection continue to exert pressure on shallow aquifers, underscoring the need for updated and systematic groundwater monitoring. To mitigate groundwater contamination, measures commonly recommended include improved wastewater treatment, better management of urban waste, and sustainable agricultural practices, which are essential to safeguard water resources and public health.

References

1. Abdelhalim A, Howard G, Howden NJK, Ahmed M, Ismail E. Carcinogenic and non-carcinogenic health risk assessment of heavy metals contamination in groundwater in the west of Minia area, Egypt. Hum Ecol Risk Assess: Int J,2003:29(2):571–596.
2. Akintola OA, Sajo OS, Olaleye OS. Assessing groundwater quality and pollution hotspots using simple fuzzy classification in a rapidly urbanizing region. Next Sustainability,2025:6:100171.
3. Alhagri MA, Al-Khashman OA, Al-Shaibani A, Al-Dhuhli H, Usman ARA. Human health risk assessment of heavy metals in groundwater resources: A case study from arid regions. Environ Sci Pollut Res,2024:31(12):16345–16359.
4. ATSDR. Toxicological profile for aluminum. Agency for Toxic Substances and Disease Registry, 2008.
5. Backman B, Bodiš D, Lahermo P, Rapant S, Tarvainen T. Application of a groundwater contamination index in Finland and Slovakia. Environ Geol,1998:36:55–64.
6. Badeenezhad A, Soleimani H, Shahsavani S, Parseh I, Mohammadpour A, Azadbakht O, *et al*. Comprehensive health risk analysis of heavy metal pollution using water quality indices and Monte Carlo simulation in R software. Sci Rep,2023:13(1):15817.
7. Bhushan C, Patel AP, Kumar A, Pandey VK, Kumar PV, Kumar P, *et al*. Hydrogeochemical characterisation and human health risk assessment of groundwater in Sultanpur District, Uttar Pradesh, India. Front Water,2025:7:1639708.
8. Bon AF, Abderamane H, Mboudou GE, Doua SA, Banakeng LA, Boyomo SBB, *et al*. Parametrization of groundwater quality of the Quaternary aquifer in N'Djamena (Chad), Lake Chad Basin: Application of numerical and multivariate analyses. Environ Sci Pollut Res,2021:28:12300–12312.
9. Cabrera F, Clemente L, Barrientos DE. Heavy metal pollution of soils affected by the Guadiamar toxic flood. Sci Total Environ,1999:242(1–3):117–129.
10. Chien SWC, Chen YC, Liu CC. Investigation of Cu and Zn into farmlands irrigated with livestock wastewaters using Nemerow pollution index. Austin J Environ Toxicol,2024:10(1):1046.

11. Dange S, Arumugam K, Vijayaraghavalu SS. Geochemical insights into heavy metal contamination and health hazards in Palar River Basin: A pathway to sustainable solutions. Ecol Indic,2024:166:112568.
12. Dashtizadeh M, Kamani H, Ashrafi SD, Panahi AH, Mahvi AH, Balarak D, *et al*. Human health risk assessment of trace elements in drinking tap water in Zahedan city, Iran. J Environ Health Sci Eng,2019:17(2):1163–1169.
13. Deubalbe D, Kadjangaba E, Bongo D, Djimouko S, Mbaigané JCD, Mahmout Y. Vulnerability evaluation of groundwater of N'Djamena City: Contribution of the parametric methods GOD and SI. J Environ Protect,2021:12:472–489.
14. Dey M, Akter A, Islam S, Chandra Dey S, Choudhury TR, Fatema KJ, *et al*. Assessment of contamination level, pollution risk and source apportionment of heavy metals in the Halda River water, Bangladesh. Heliyon,2021:7(12):e08625.
15. Djoret D. Etude de la recharge de la nappe du Chari Baguirmi (Tchad) par lesméthodes chimiques et isotopiques. Thèse, Université d'Avignon et des Pays du Vaucluse, 2000.
16. Doumnang Mbaigané JC. Cartographie des marécages de la ville de N'Djamena (Tchad) à partir d'images satellitaires. Rapport CORUS/15/2005, Université de N'Djamena, 2005.
17. Edet AE, Offiong OE. Evaluation of water quality pollution indices for heavy metal contamination monitoring: A case study from Akpabuyo-Odukpani Area, Lower Cross River Basin (Southeastern Nigeria). Geomicrobiol J,2002:19:295–304.
18. Edith K, Alhabib IM, Léontine T, Djimako B, Jean-Claude DM. Evaluation of quality of water from wells and boreholes located in some irrigated perimeters of N'Djamena city: Case of sites of Digangali, Moursal, Sabangali and Walia. J Mater Environ Sci,2022:13(12):1446–1455.
19. Egbueri JC. Heavy metals pollution source identification and probabilistic health risk assessment of shallow groundwater in Onitsha. Anal Lett,2020:53:1620–1638.
20. EPA. Risk Assessment Guidance for Superfund: Volume I — Human Health Evaluation Manual (Part A, Baseline Risk Assessment) (EPA/540/1-89/002). Office of Emergency and Remedial Response, U.S. Environmental Protection Agency, Washington, DC, 1989.
21. EPA. Exposure Factors Handbook: 2011 edition, (Final Report). (EPA/600/R-09/052F). U.S. Environmental Protection Agency, Washington, DC, 2011.
22. EPA. Provisional Peer-Reviewed Toxicity Values For Rubidium Compounds (Rubidium). U.S. Environmental Protection Agency, Washington, DC, EPA/690/R-16/012F,2016.
23. EPA. Integrated Risk Information System (IRIS), List of Substances A to Z. U.S. Environmental Protection Agency, Washington, DC, 2025.
24. EWG. Cobalt – Tap Water Database. Environmental Working Group City of Ontario, 2023.
25. Finley BL, Monnot AD, Paustenbach DJ, Gaffney SH. Derivation of a chronic oral reference dose for cobalt. Regul Toxicol Pharmacol,2012:64(3):491–503.
26. Gong Q, Deng J, Xiang Y, Wang Q, Yang L. Calculating pollution indices by heavy metals in ecological geochemistry assessment and a case study in parks of Beijing. J China Univ Geosci,2008:19:230–241.
27. Guideal R, Bala AE, Ikpokonte EA. Physical and Chemical Quality of Groundwater in the Quaternary Aquifer in N'djamena Region, Chad Republic. J Appl Sci Res,2010:6(11):1885–1890.
28. Gwira HA, Osae R, Abasiya C, Peasah MY, Owusu F, Loh SK, *et al*. Hydrogeochemistry and human health risk assessment of heavy metal pollution of groundwater in Tarkwa, a mining community in Ghana. Environ Adv, 2024, 17.
29. Han Z, Ma H, Shi G, *et al*. A review of groundwater contamination near municipal solid waste landfill sites in China. Sci Total Environ,2016:569:1255–1264.
30. Idriss Mahamat Y, Mahamat Nour A, Rozzi Kelleymi K, Abderamane H. Assessment of Industrial Impact on Groundwater Quality in N'Djamena, Chad. Pak J Anal Environ Chem,2024:25(2):293–305.
31. Kadjangaba E. Etude hydrochimique et isotopique du système zone non saturée–nappe dans la zone urbaine de N'Djamena: Impact de la pollution. Thèse de doctorat, Université d'Avignon et des Pays du Vaucluse, 2007.
32. Kadjangaba E, Huneau F, Travi Y, Djoret D. Recharge and Groundwater Quality of an Alluvial Aquifer: Case of the City of N'djamena (Chad). J Environ Sci Eng B,2017:6:493–505.
33. Kadjangaba E, Djoret D, Doumnang Mbaigané JC, Ndoutamia Guelmbaye A, Mahmout Y. Impact des Processus Hydrochimique sur la Qualité des Eaux souterraines de la Ville de N'Djamena-Tchad. Eur Sci J,2018:14:162–177.
34. Kudamnya EA, Edet AA. Comparison assessment of trace and rare earth elements concentration and associated health risk in groundwater from northcentral and southeastern Nigeria. Arab J Geosci,2024:17:86.
35. Kumar S, Maurya NS. Analysis of heavy metal contamination in groundwater and associated probabilistic human health risk assessment using Monte Carlo simulation: A case study in Gaya, Bihar. J Water Health,2025:23(5):630–647.
36. Li MS, Yang SX. Heavy metal contamination in soils and phytoaccumulation in a manganese mine Wasteland, South China. Air Soil Water Res,2008:1:31–41.
37. Liu Y, Yu H, Sun Y, Chen J. Novel assessment method of heavy metal pollution in surface water: a case study of Yangping River in Lingbao City, China. Environ Eng Res,2017:22:31–39.
38. Louis P. Contribution géophysique à la connaissance géologique du bassin du lac Tchad. ORSTOM, Paris, 1970.
39. Luo YS, Azores JPC, Reyes RM, Apostol GLC. Probabilistic human health risk assessment of inorganic arsenic exposure following the 2020 Taal Volcano eruption, Batangas, Philippines. Toxics,2026:14(1):13.
40. Mandal BK, Suzuki KT. Arsenic round the world: A review. Talanta,2002:58(1):201–235.
41. Maskooni EK, Naseri-Rad M, Berndtsson R, Nakagawa K. Use of heavy metal content and modified water quality index to assess groundwater quality in a semiarid area. Water,2020:12(4):1115.

42. MDH. Strontium and groundwater – Health advisory levels. Minnesota Department of Health,2019. https://www.health.state.mn
43. Meng J, Xiao G, Qi M, Han X, Gou Q, Hao X, Ge J. Comparing roles of multiple contamination indicators in tracing groundwater pollution nearby a typical municipal solid waste (MSW) landfill. Heliyon,2024:10(16):e35601.
44. Miletic A, Lucic M, Onjia A. Exposure factors in health risk assessment of heavy metal(loid)s in soil and sediment. Metals,2023:13:1266.
45. Mohan SV, Nithila P, Reddy SJ. Estimation of heavy metals in drinking water and development of heavy metal pollution index. J Environ Sci Health A,1996:31(2):283–289.
46. Moussa A, Mahamat Nour A, Abderamane H, Abdel-Aziz AY. Geological and Hydrogeological Structure of the Aquifer of the City of N'djamena, Chad. Res J Environ Earth Sci,2020:12(3):53–63.
47. NHMRC. Australian drinking water guidelines paper 6: National water quality management strategy. National Health and Medical Research Council, 2011.
48. NSF. Rubidium (CAS # 7440-17-7) – Oral risk assessment document. NSF International, Ann Arbor, Michigan, 2018.
49. OEHHA. Technical support document for cancer potency factors. California Environmental Protection Agency, 2009.
50. OEHHA. Proposed notification level for vanadium. California Office Environmental Health Hazard Assessment, 2021.
51. Schneider JL, Wolff JP. Carte géologique et Hydrogéologique au 1/1 500 000 de la République du Tchad. Mémoire explicatif. Document BRGM, 1992, 209(1,2).
52. Shakoor H, Alshehri F, Shahab M, Abanumay FA, Ali L. Vulnerability and risk assessment of lead (Pb) concentrations in drinking water via statistical and geostatistical analyses. Front Water,2025:7:1548110.
53. Singh A, Chaudhary S, Dehiya BS. Spatial Variations of Heavy Metal Content in the Surface Water of Yamuna River, India. Appl Ecol Environ Sci,2020:8(5):244–25.
54. Stephen H, Bassi W, Sirante R, Alli RM. Health risk assessment of heavy metals in water sources from selected regions in Yola North, Adamawa State, Nigeria. J Multidiscip Sci: Mikailalsys,2024:2(3):452C467.
55. Su K, Wang Q, Li L, Cao R, Xi Y, *et al*. Water quality assessment based on Nemerow pollution index method: A case study of Heilongtan reservoir in central Sichuan province, China. Plos One,2022:17(8):e0273305.
56. Taylor AA, Tsuji JS, McArdle ME, Adams WJ, Goodfellow WL Jr. Recommended Reference Values for Risk Assessment of Oral Exposure to Copper. Risk Anal,2023:43(2):211–218.
57. Tekoum L, Moussa AD, Bichara L, Hamid A. Effects of Latrines on Water Quality in the Phreatic Nappe in N'Djamena City: (5th District), Chad. J Water Resour Protect,2024:16(12):793–810.
58. Tiwari D, Kumar R, Yadav M, Gupta GK, Singh SK, Dhapekar NK, Alotaibi MA, Sharma R. Holistic analysis of Ganga basin water quality: A statistical approach with WQI, HMCI, HMQI and HRI indices. RSC Adv,2025:15(5):3290–3316.
59. Vicat JP, Doumnang Mbaigané JC. Estimating drinking-water ingestion requirements under hot climate conditions: The case of N'Djamena (Chad). Int J Ecol Environ Sci,2025:7(4):117–119.
60. Wang S. Environmental occurrence, transformation, and toxicity of organoarsenic compounds: A review. Chemosphere,2022:287:131958.
61. Wator K, Kmiecik E, Michalik A, Kowalczyk A. Human health risk assessment of trace elements in tap water and the factors influencing its value. Int J Environ Res Public Health,2021:18(4):1713.
62. WHO. Arsenic and arsenic compounds (2nd ed.). World Health Organization, 2001.
63. WHO. Guidelines for drinking-water quality: Fourth edition incorporating the first and second addenda. World Health Organization, 2022.
64. Yan N, Liu W, Xie H, Gao L, Han Y, Wang M, Li H. Distribution and assessment of heavy metals in the surface sediment of Yellow River, China. J Environ Sci (China),2016:39:45–51.
65. Zakir HM, Sharmin S, Akter A, Rahman MS. Assessment of health risk of heavy metals and water quality indices for irrigation and drinking suitability of waters: A case study of Jamalpur Sadar Area, Bangladesh. Environ Adv,2020:2:100005.
66. Zhaoyong Z, Abuduwaili J, Fengqing J. Heavy metal contamination, sources, and pollution assessment of surface water in the Tianshan Mountains of China. Environ Monit Assess,2015:187:33.